



Effect of processing variables on the reaction kinetics of MgB₂ fibers

John D. DeFouw*, David C. Dunand

Department of Materials Science & Engineering, Northwestern University, Evanston, IL 60208, USA

ARTICLE INFO

Article history:

Received 1 April 2010

Accepted 7 June 2010

Available online 10 June 2010

Keywords:

Reaction kinetics

X-ray diffraction

Magnesium diboride

Thermal cycling

ABSTRACT

The reaction kinetics for converting B fibers into MgB₂ fibers are measured by *in situ* synchrotron X-ray diffraction and *ex situ* by metallography as a function of the following processing variables: fiber diameter, fiber doping, fiber surface treatment, Mg flux (liquid or gaseous Mg), and thermal cycling. Changes to the fiber diameter, surface treatment and Mg flux affect little the rates of the reaction, while C-doping of fibers dramatically decreases reaction rate and thermal cycling increases the reaction rate.

© 2010 Elsevier B.V. All rights reserved.

1. Introduction

The boride MgB₂ is a promising new superconducting material due to its combination of relatively high transition temperature ($T_c = 39$ K), lack of weak link behavior at grain boundaries, low cost of elements, and ease of synthesis from the elements [1]. The reaction kinetics for synthesis of MgB₂ from elemental Mg and B:



have been studied between Mg vapor and a B thin film [2] and between Mg and B powders [3–6], and take place via the creation of intermediate borides (mainly MgB₄ and very little MgB₇). The reaction is described as a diffusional process with temperature as the primary parameter to alter the reaction kinetics. By measuring reaction rates as a function of temperature and modeling the geometry of the powders or film, the reaction kinetic parameters (i.e., diffusion coefficients, rate constants, and activation energies) were determined [2,3]. Recently, the analysis was extended to reacting B fibers and liquid Mg to MgB₂ fibers [7] where the large diameter of the B fibers (140 μm) and extensive reaction volume expansion (90% volume increase from B to MgB₂) induced cracking during synthesis, which increased the surface area and thus accelerated the diffusion controlled MgB₂ synthesis reaction [7]. In that study, the only processing variable studied was temperature.

In the present paper, we study additional processing parameters affecting the reaction of B fibers into MgB₂: B fiber size (100 vs. 140 μm), Mg flux (Mg vapor vs. Mg liquid), surface of the B fibers (with and without a thin nitride layer), chemistry of B fibers (with and without doping with 0.4 at.% C), temperature profile

(isothermal vs. thermal cycling) and fiber length (continuous vs. fragmented). This systematic study allows the identification of the parameters affecting the MgB₂ synthesis kinetics.

2. Material and methods

The reaction of B fibers immersed within liquid Mg was studied *in situ* by synchrotron diffraction, as described elsewhere [3,7]. In brief, bundles of 20 mm long B fibers were first pressure infiltrated with liquid Mg inside a titanium crucible. The sample was later heated under Ar cover gas to the reaction temperature in a custom furnace, while a high energy X-ray beam passed through the sample and produced a diffraction pattern on a CCD camera. Through measuring diffraction intensity with time, the kinetics of the reaction were determined. Here, several experiments were conducted to investigate the effects of various parameters on reaction rates and MgB₂ microstructure. First, 100 μm diameter B fibers (from Specialty Materials, Inc., Lowell, MA) were reacted in liquid Mg at 900–1000 °C and compared to data on 140 μm diameter B fibers (from Specialty Materials, Inc., Lowell, MA) collected in previous research [7]. Second, the above 100 μm B fibers were also reacted at 900–1000 °C with Mg vapor, with a flux related to the vapor pressure of Mg reduced as compared to experiments with liquid Mg carried out at the same temperatures. Third, fibers of 140 μm diameter (from AVCO, with similar W fiber core) with a thin 1–2 μm outer nitride coating created by first oxidizing the fiber then reacting with ammonia [8] were reacted in liquid Mg at 900–1000 °C and compared with previous data on uncoated 140 μm B fibers [7]. In a fourth series of experiments, 85 μm diameter B fibers doped with 0.4 at.% C – synthesized by Specialty Materials, Inc. through decomposition of CH₄ and BCl₃ during the chemical vapor deposition (CVD) on a W fiber [9] – were studied *ex situ* by

* Corresponding author.

E-mail address: jdefouw@u.northwestern.edu (J.D. DeFouw).

metallography after reaction at 1000 °C for 5 min and 2.5 h in liquid Mg to investigate the effect of C upon reaction rate.

The low surface to volume ratio of continuous B fibers with >100 μm diameter slows their reaction rate as compared to the much finer B powders studied to date [3]. One possible path to improve reaction rate of fibers is to enhance, during the reaction, cracking of the boride layer growing radially into the B fiber by exploiting the differences in thermal expansion between the unreacted boron and the growing boride layer. To this end, reaction rates between liquid Mg and 140 μm B fibers were measured under thermal cycling conditions, and compared to baseline isothermal conditions. The temperature was cycled across 668–900 °C ($\Delta T = 232$ °C) and 737–900 °C ($\Delta T = 163$ °C) while isothermal baseline experiments were conducted at the upper temperature of 900 °C. The cycles were approximately square with near linear cooling to the lower temperature in 1 min followed immediately by heating back to 900 °C in 1 min where it was then held for 28 min (30 min period, 10 cycles) or 8 min (10 min period, 30 cycles) resulting in 5 h total reaction time. Finally, to investigate the geometrical effect associated to the continuous nature of the fibers, 100 μm B fibers were mechanically fractured into 25–45 μm fragments which were reacted with liquid Mg at 900 °C and compared to continuous fiber reactions at the same temperature. Also, for comparison, large (60–140 μm) irregular crystalline B powders (form Alfa Aesar, Ward Hill, MA) were reacted at 800 °C for 2 h in liquid Mg and imaged using optical microscopy.

3. Results and discussion

3.1. Fiber diameter

Fig. 1 shows reaction kinetic plots for 100 μm diameter B fibers, where the degree of reaction is plotted as a function of reaction time. The reaction rate decreases monotonically with time, and reaction is completed in ~1 h at 1000 °C, ~2 h at 950 °C and ~4.5 h at 900 °C. Times to achieve full reaction were similar to those previously measured on 140 μm diameter fibers, despite the higher volume (by a factor two) of the latter fibers. By contrast, the Entchev diffusion model presented in Refs. [3,7,10], which assumes a reaction front progressing radially in the B fiber without

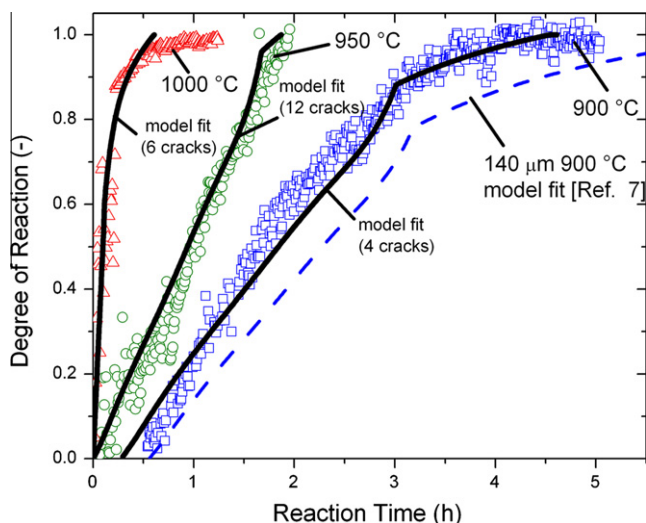


Fig. 1. Degree of reaction vs. time plot for 100 μm B fibers reacted in liquid Mg between 900 and 1000 °C with diffusion and cracking model fits using diffusion coefficients within the uncertainty measured in previous research [7]. A dashed line of the fit of the reaction of larger 140 μm diameter fibers [7] is shown for comparison.

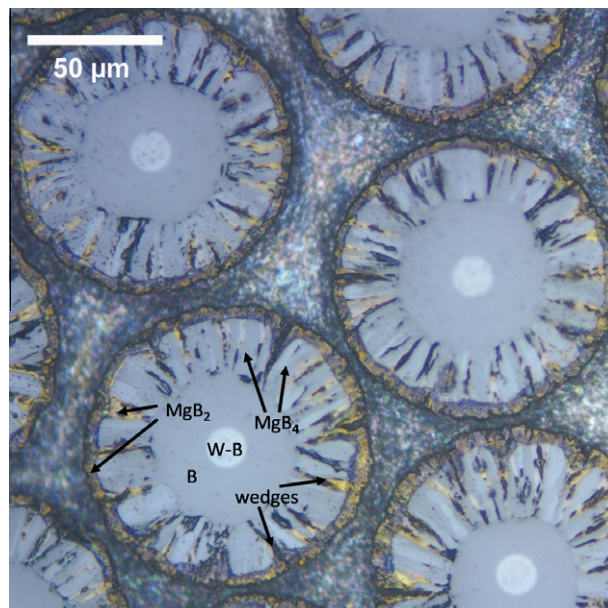


Fig. 2. Optical micrograph showing cross-sections of 100 μm B fibers reacted for 3 min at 1000 °C.

cracking, predicts that a 100 μm diameter B fiber reacts to MgB₂ in 51% of the time needed for a 140 μm B fiber to fully react. This model predicts much longer reaction times than experimentally observed here, because it does not take into account the cracking of the reaction layer, observed in previous experiments with 140 μm B fiber [7] and in the present experiments (Fig. 2), which increases the area of the fiber available for reaction and thus decreases reaction times.

A more complex model taking into account reaction layer cracking [7] also predicts complete reaction of the smaller 100 μm diameter B fiber in about half the time of the larger 140 μm B fiber, assuming that the fibers contain four cracks and choosing diffusion coefficients which fit the curves shown in Fig. 1. In this figure, fits of this cracking model to reaction kinetics data of 100 μm B fibers at 900 °C are best achieved with the following parameters: number of cracks: $N = 4$; MgB₂ diffusion coefficient: $D_{\text{MgB}_2} = 6 \times 10^{-14} \text{ m}^2 \text{ s}^{-1}$; MgB₄ diffusion coefficient: $D_{\text{MgB}_4} = 5 \times 10^{-13} \text{ m}^2 \text{ s}^{-1}$; and a shift of 18 min to account for some incubation time. Similarly, 1000 °C data for reaction of 100 μm B fibers are best fit with $N = 6$, $D_{\text{MgB}_2} = 1 \times 10^{-12} \text{ m}^2 \text{ s}^{-1}$, and $D_{\text{MgB}_4} = 12 \times 10^{-12} \text{ m}^2 \text{ s}^{-1}$. Finally, the 950 °C reaction curve of 100 μm fibers is best fit by $N = 12$, $D_{\text{MgB}_2} = 8 \times 10^{-14} \text{ m}^2 \text{ s}^{-1}$, and $D_{\text{MgB}_4} = 8 \times 10^{-13} \text{ m}^2 \text{ s}^{-1}$. All three fits are plotted in Fig. 1 and the parameters for the fits are close those found in a previous study for 140 μm diameter fibers [7]. A relatively high number of cracks is needed to fit the very linear nature of the experimental reaction curve. As discussed in Ref. [7], the curves typically have a transition from a fast to a slower reaction rate which corresponds to the point where MgB₂ wedges growing radially in the fiber meet its center and radial circumferential diffusion becomes the sole active mechanism. With a high number of cracks, the curves become more linear since more of the fiber is reacted by the radial crack mechanism, resulting in less material being reacted by the slower diffusion mechanism.

The microstructure of the 100 μm diameter fibers reacted at 1000 °C for 3 min is shown in Fig. 2 and is similar to that found for 140 μm diameter fibers [7]. The reaction layer consists of an outer ring of MgB₂ and an intermediate layer of MgB₄ and the extents of the reaction fronts (4 and 22 μm, respectively) are similar to those reported previously for 140 μm fibers [7]. In both cases,

the MgB_4 layer shows radial cracks in which MgB_2 is growing as wedges [7]. As the reaction progresses, the cracks merge and their number decreases, so that the best fit $N = 6$ found above is credible. That both fibers, despite their different diameter, require similar times to achieve full conversion to MgB_2 may be explained by a smaller number of cracks (due to lower crack nucleation or early crack merging) for the thinner fibers, so that the specific area exposed for the reaction is similar.

3.2. Magnesium flux

Fig. 3 shows the reaction kinetics of 100 μm B fibers exposed to gaseous Mg at temperatures between 900 and 1000 $^\circ\text{C}$. There is no obvious difference in kinetics as compared to reaction in liquid Mg, as illustrated in Fig. 3. At the high temperatures used here, the Mg vapor pressure ranges from 0.2 atm at 900 $^\circ\text{C}$ to 0.64 atm at 1000 $^\circ\text{C}$ [11]. The similarity of the kinetics data for reactions occurring with liquid and vapor Mg suggests that the Mg flux in the vapor between 900 and 1000 $^\circ\text{C}$ is sufficient to achieve the maximum possible reaction rate, and that another step in the reaction, e.g., diffusion in the fiber, is rate-limiting.

3.3. Nitride coating of fibers

Reaction kinetics for nitride coated 140 μm B fibers are shown in Fig. 4 and are roughly similar to those for non-coated fibers, except for an incubation time during which reaction proceeded very slowly, before the onset of fast reaction to completion. This incubation time is short (<10 min) for reactions at 950–1000 $^\circ\text{C}$, but increases to ~ 30 min for 925 $^\circ\text{C}$ and ~ 1 h for 900 $^\circ\text{C}$ reaction. The nitride coating was visible as a lighter shade in backscattered SEM and was ~ 2 μm thick (Fig. 5). Nitriding of B fibers was developed to prevent reaction of the B fibers during infiltration with liquid Al but Mg forms stable nitrides according to the Mg–N phase diagram [12], so it is not unexpected that the reaction can proceed. The present data indicates that the nitride coating provides partial protection against reaction with liquid Mg, which improves as the temperature decreases from 1000 to 900 $^\circ\text{C}$.

3.4. Carbon doping of fibers

The thickness of the MgB_2 reaction shells for 85 μm B fibers doped with 0.4 at.% C is 1.6 μm after 3 min exposure to liquid Mg

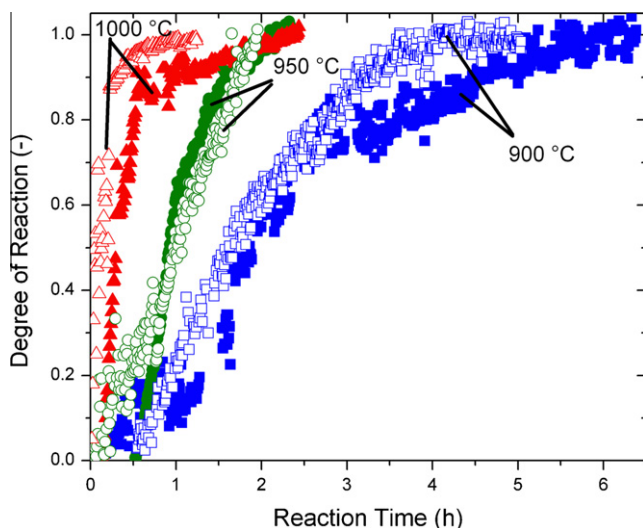


Fig. 3. Degree of reaction vs. time plots for reaction of 100 μm B fibers at 900, 950 and 1000 $^\circ\text{C}$ in Mg vapor (closed symbols) and in Mg liquid (open symbols).

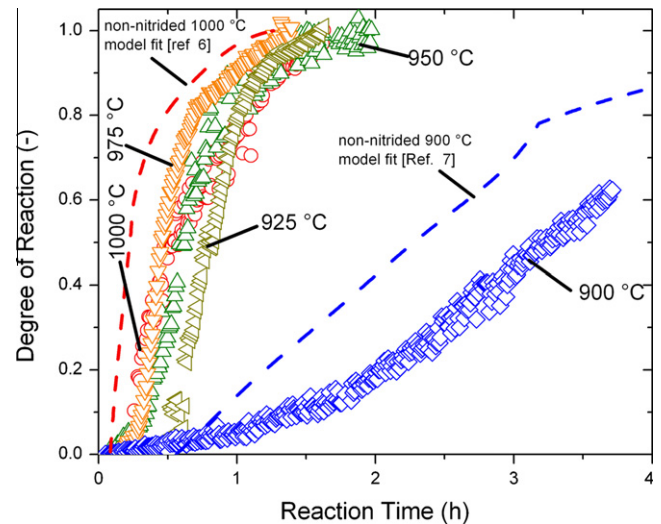


Fig. 4. Degree of reaction vs. time plots for 140 μm B fibers with nitrided surface reacted between 900 and 1000 $^\circ\text{C}$ in Mg liquid. Dashed lines of fits of 140 μm non-nitrided B fibers from Ref. [7] shown for comparison.

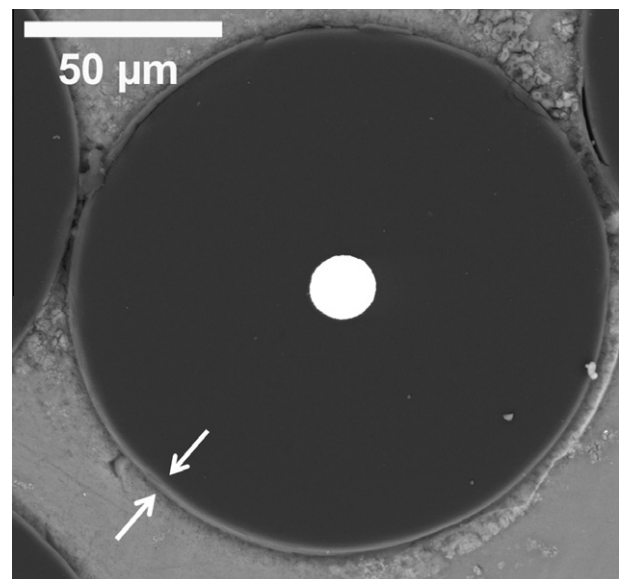


Fig. 5. Scanning electron micrograph of cross-section of unreacted 140 μm B fiber in a magnesium matrix with lighter shaded nitride ring on the outer edge of the fiber. The nitride layer was determined to be 1.8–2.2 μm thick on higher magnification micrographs.

at 1000 $^\circ\text{C}$ (Fig. 6a), as compared to ~ 4 μm for 100 μm un-doped fibers (Fig. 2). The MgB_2 reaction depth increases slowly to 3.6 μm after 2.5 h and to 3.9 μm after 16.5 h, as shown in Fig. 6b and c. In contrast, un-doped 100–140 μm B fibers fully reacted in 2.5 h at 950–1000 $^\circ\text{C}$ [7,13,14]. Fit of the Entchev model [3,7,10] as shown in Fig. 7 to these three data points resulted in a diffusion coefficient of $1.4 \times 10^{-15} \text{ m}^2 \text{ s}^{-1}$, which is much less than the diffusion coefficient of $9 \times 10^{-13} \text{ m}^2 \text{ s}^{-1}$ found for the un-doped fibers [7]. The fit is very rough, so the value of the diffusion coefficient is approximate, but the two to three orders of magnitude difference is probably correct. The MgB_4 reaction front was absent in doped fibers, unlike for the un-doped fibers at 1000 $^\circ\text{C}$, but similar to un-doped fibers at 700 and 800 $^\circ\text{C}$ temperatures, which have similarly slower diffusion coefficients [7]. Reactions of C-doped B fibers have been reported to occur much slower than the reaction

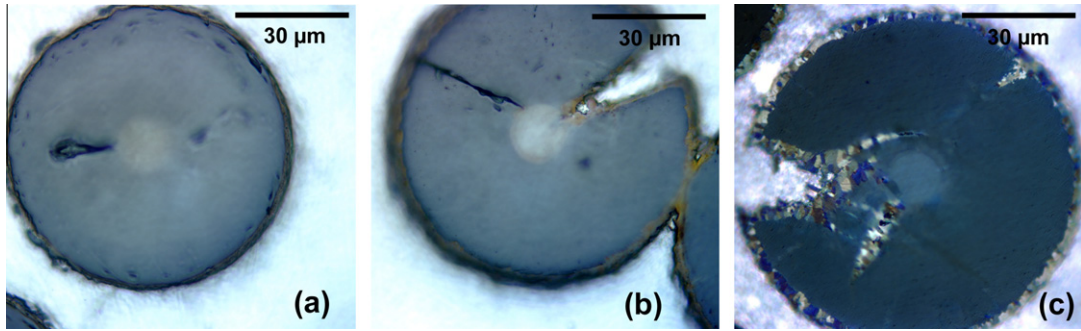


Fig. 6. Optical micrographs showing cross-sections of C-doped 85 μm B fibers reacted in Mg liquid at 1000 °C for (a) 5 min, (b) 2.5 h, and (c) 16.5 h.

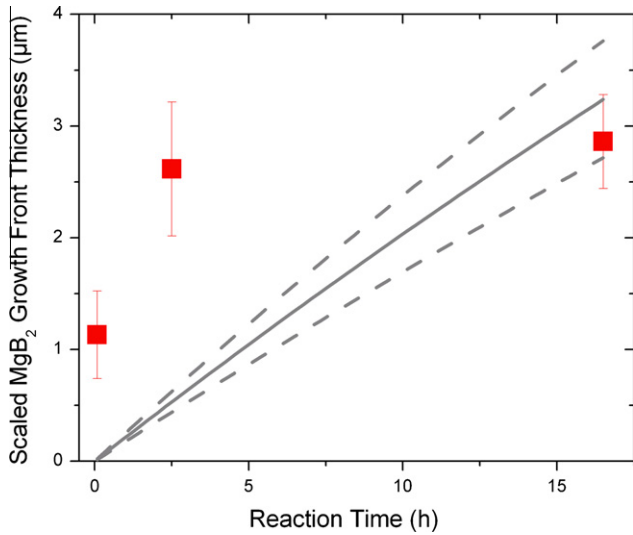


Fig. 7. Plot of MgB₂ thickness vs. time for C-doped 85 μm B fibers reacted in liquid Mg at 1000 °C. Lines show predictions of Entchev et al. [10] cylinder reaction model.

of un-doped B fibers with reactions completed in 72 h at 1000 °C or 48 h at 1200 °C [15].

Possible explanations for the much slower reaction of C-doped fibers include formation of B₄C, reduction of the cracking mechanism, and/or improved adhesion of interfaces similar to the effect of rare-earth elements on oxide layers in alloys such as Fe–Cr–Al. Long reaction times at high temperatures were reported for the reaction of B₄C to carbon-doped MgB₂ [16,17] as well as the reaction of Ti- and C-doped fibers [9,15,18,19]. B₄C is a highly stable carbide which resists reaction to MgB₂, but no B₄C was reported for the synthesis of C-doped B fibers by CVD [9]. The cracking of C-doped fibers was not observed, but this was likely due to slow diffusion and growth of the MgB₄ front. Similar reaction fronts were shown with slow diffusion coefficients at 700 and 800 °C in undoped fibers [7]. The addition of a small amount of Y and other rare-earth elements to Fe–Cr–Al, and other alumina and chromia forming alloys, which improves adhesion between alloy and oxide layers and resists cracking, thus preventing the additional diffusion of oxygen to fully oxidize the alloys [20]. The diffusion of Mg in reacting B fibers to MgB₂ may follow a similar process. If C-doping follows a similar mechanism, it could slow or even prevent the diffusional process, thus slowing the reaction rate. Addition of Y changes oxide growth in Fe–Cr–Al alloys from parabolic to near asymptotic where oxidation proceeds early and then nearly stops, as seen here where reaction thickness at 16.5 h was similar to the reaction thickness after 2.5 h, within the experimental error of 0.5 μm. This also ex-

plains why it was previously found [3] that C-doped powders show no decrease in reaction times as compared to un-doped powders. In that study, B powder agglomerates were only 400 nm in size and consisted of 10–50 nm B particles, much below the 1.6 μm thick shell of MgB₂ created after only 3 min reaction at 1000 °C shown in Fig. 6a.

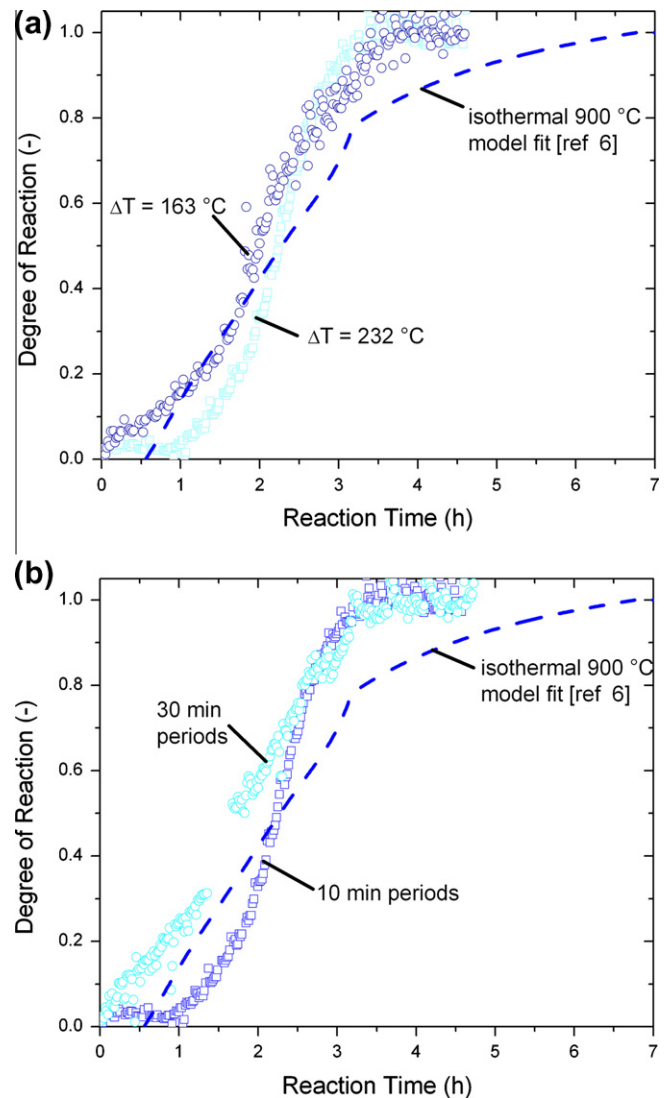


Fig. 8. Degree of reaction vs. time plots comparing different thermal cycling conditions for 140 μm B fibers in Mg liquid. (a) Effect of cycle amplitude (ΔT) on reaction and (b) effect of cycle period on reaction. Thermal cycling decreased the overall reaction time by enhancing the cracking in the fibers as shown in comparison to the isothermal reaction shown with dashed lines.

3.5. Thermal cycling

Fig. 8 shows reaction kinetics of 140 μm B fibers reacted with liquid Mg under 668–900 $^{\circ}\text{C}$ thermal cycling conditions and compared isothermal reaction at 900 $^{\circ}\text{C}$. Thermal cycling had no noticeable effect for up to $\sim 80\%$ degree reaction. Beyond that point, however, thermal cycling noticeably accelerated kinetics, reducing time to reach full reaction by a factor two, from ~ 7 h to ~ 3.5 h. This later stage of reaction corresponds to the point where MgB_2 wedges (formed at the cracks visible in Fig. 2) reach the fiber core and reaction occurs by lateral spreading of these wedges consuming remnants of MgB_4 “islands” [7]. Thus, it appears that thermal cycling aids in enhancing cracking of these MgB_4 regions due to thermal mismatch, thereby accelerating the last conversion of MgB_4 to MgB_2 . Changes to the cycling conditions, including cycle amplitude (ΔT) as well as cycle period, affected somewhat the kinetic curves

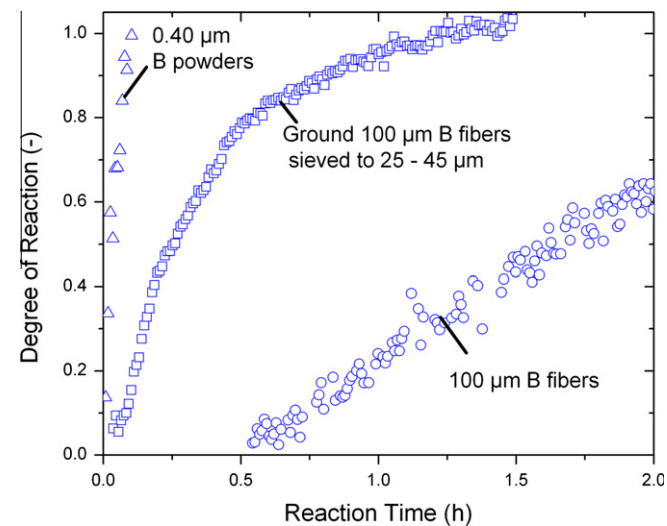


Fig. 9. Degree of reaction vs. time plot showing 100 μm diameter B fibers that were ground and sieved to 25–45 μm and reacted in liquid Mg at 900 $^{\circ}\text{C}$. Reactions of unbroken 100 μm diameter cylindrical B fibers and 0.40 μm B powders [3] are shown for comparison.

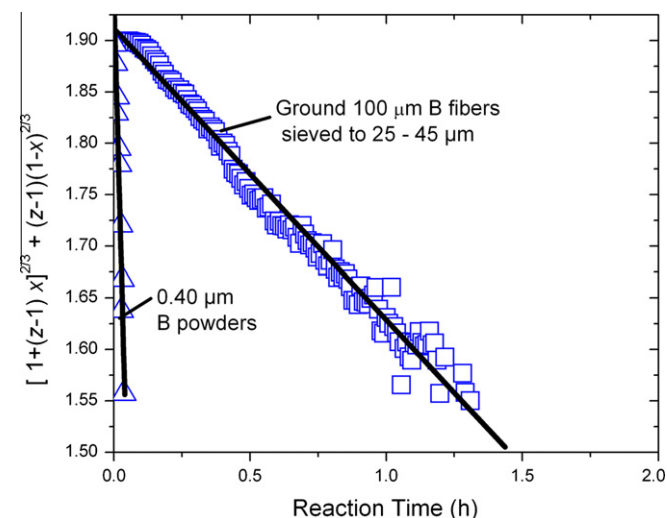


Fig. 10. Degree of reaction vs. time plot for data in Fig. 9 (25–45 μm ground B fibers and 0.40 μm B powders) converted to the Carter sphere model [21] where z is the volumetric expansion of B converting to MgB_2 ($z = 1.90$) and x is the degree of reaction. The best-fit slopes are related to the reaction rate constant k [3].

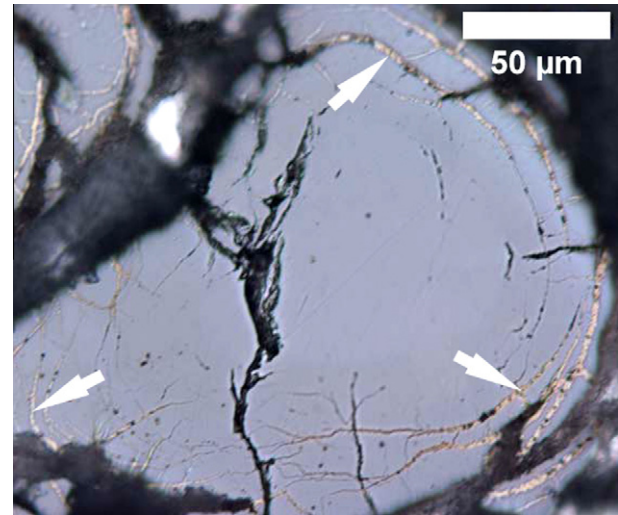


Fig. 11. Optical micrograph of cross-section of large crystalline B powders (60–140 μm) reacted with liquid Mg at 800 $^{\circ}\text{C}$ for 2 h with arrows indicating regions where MgB_2 grew into cracked regions within a single particle.

but had little effect on the time to achieve full reaction, as shown in Fig. 8a and b. These results indicate that thermal cycling near the end of the synthesis process, rather than over the whole process, is sufficient to shorten the reaction time of the fibers.

Thermal cycling experiments were also carried out between 700 and 1000 $^{\circ}\text{C}$ for 24 h on C-doped fibers but did not result in enhancement of reaction rate. This is likely due to the lack of an MgB_4 reaction front (Fig. 6) so the cracking mechanism observed previously [7] and discussed above for the un-doped fibers cannot be activated.

3.6. Fractured fibers

As shown in Fig. 9, fragments of 100 μm B fibers fully reacted in liquid Mg at 900 $^{\circ}\text{C}$ in ~ 1.5 h, in a third of time (4.5 h) needed for intact fibers. These fragments were sieved to 25–45 μm and thus resembled coarse powders, so the reaction curves were well fit by the Carter sphere reaction model previously used for much finer B powders [3,21], as shown in Fig. 10. Using the characteristic radii r_0 of 12.5–22.5 μm as lower and upper bounds, the reaction rate constant from the Carter model was determined to be between 6.8×10^{-15} and $2.2 \times 10^{-14} \text{ m}^2 \text{ s}^{-1}$. These reaction rate constants are at least an order of magnitude larger than found previously for 400 nm powders at 900 $^{\circ}\text{C}$ [3]. It is likely that this enhancement is due to cracking. Indeed, MgB_2 was observed growing into cracks in large crystalline B powders (60–140 μm) reacted at 800 $^{\circ}\text{C}$ for 2 h, as shown in Fig. 11. By contrast, the 400 nm B powders were probably too fine for the cracking mechanism to be operative.

4. Conclusions

The conversion of B fibers to MgB_2 fibers was studied both *in situ* (by synchrotron X-ray diffraction) and *ex situ* (by metallography) as a function of the following parameters:

1. Temperature: kinetics increase with temperature between 900 and 1000 $^{\circ}\text{C}$, in quantitative agreement with an existing model considering diffusional growth into the B fiber of a smooth MgB_4 layer, which is subsequently converted to MgB_2 through radial cracks increasing the surface area available for reaction.
2. B fiber diameter: fibers with 100 μm diameter achieve full reaction in similar time to fibers with 140 μm diameter, despite a

50% difference in volume. This is probably due to a lower number of cracks.

3. B fiber continuity: fragmented fibers achieved full reaction in a third of the time for intact fibers at 900 °C, because of lower diffusion distance needed. Growth of MgB₂ at cracks is occurring, as in intact B fibers and large B particles, but unlike sub-micrometer B powders.
4. B fiber surface treatment: a thin nitride layer on the B surface affects kinetics through an incubation time, which becomes important for the lowest studied temperature of 900 °C.
5. B fiber doping: doping of the fiber with 0.4 at.% C dramatically decreased reaction rates, as previously observed [15]. This effect is associated with the lack of formation of a MgB₄ layer and its subsequent cracks which enables rapid MgB₂ growth.
6. Mg flux: as reaction rates were similar for fibers exposed to liquid or gaseous Mg, reactant transport to the fiber is not rate controlling over the 900–1000 °C range.
7. Thermal profile: thermal cycling enhanced reaction kinetics in the latter stage of reaction, most probably through enhanced cracking of the MgB₄ layer by thermal mismatch stresses, halving the time to reach full reaction as compared to isothermal reaction. This improvement was not achieved in C-doped fibers due to the lack of a MgB₄ growth front.

Acknowledgements

This work was supported by the US National Science Foundation through Grant No. DMR-0319051. The authors thank Dr. J. Marzik of Specialty Materials, Inc. for providing C-doped and undoped B fibers and Drs. J. Quintana, Q. Ma and D. Keane for help in performing the diffraction experiments at the DuPont-North-

western-Dow Collaborative Access Team (DND-CAT). DND-CAT is supported by E.I. DuPont de Nemours & Co., The Dow Chemical Company and the State of Illinois and is located at Sector 5 of the Advanced Photon Source which is supported by the US Department of Energy under Contract No. DE-AC02-06CH11357.

References

- [1] P.C. Canfield, S.L. Bud'ko, D.K. Finnemore, *Physica C* 385 (2003) 1.
- [2] H.M. Kim, S.S. Yim, K.B. Kim, S.H. Moon, Y.W. Kim, D.H. Kang, *J. Mater. Res.* 19 (2004) 3081.
- [3] J.D. DeFouw, D.C. Dunand, J.P. Quintana, *Acta Mater.* 56 (2008) 1680.
- [4] A.N. Baranov, V.L. Solozhenko, C. Lathé, V.Z. Turkevich, Y.W. Park, *Supercond. Sci. Technol.* 16 (2003) 1147.
- [5] J.C. Grivel, R. Pinholt, N.H. Andersen, P. Kovac, I. Husek, J. Homeyer, *Supercond. Sci. Technol.* 19 (2006) 96.
- [6] S. Yan, Y. Lu, G. Liu, G. Yan, L. Zhou, *J. Alloys Compd.* 443 (2007) 161.
- [7] J.D. DeFouw, D.C. Dunand, *Acta Mater.* 56 (2008) 5751.
- [8] B. Jacob, R. Bordeuau, F. Galasso, *Fibre Sci. Technol.* 1 (1969) 243.
- [9] R.H.T. Wilke, S.L. Bud'ko, P.C. Canfield, D.K. Finnemore, R.J. Suplinskas, S.T. Hannahs, *Phys. Rev. Lett.* 92 (2004) 217003.
- [10] P.B. Entchev, D.C. Lagoudas, J.C. Slattery, *Int. J. Eng. Sci.* 39 (2001) 695.
- [11] R.E. Honig, D.A. Kramer, *RCA Rev.* 30 (1969) 285.
- [12] T.B. Massalski, *ASM International, Binary Alloy Phase Diagrams*, 2nd ed., ASM International, Materials Park, Ohio, 1990.
- [13] J.D. DeFouw, D.C. Dunand, *Appl. Phys. Lett.* 83 (2003) 120.
- [14] P.C. Canfield, D.K. Finnemore, S.L. Bud'ko, J.E. Ostenson, G. Lapertot, C.E. Cunningham, C. Petrovic, *Phys. Rev. Lett.* 86 (2001) 2423.
- [15] R.H.T. Wilke, S.L. Bud'ko, P.C. Canfield, M.J. Kramer, Y.Q. Wu, D.K. Finnemore, R.J. Suplinskas, J.C. Marzik, S.T. Hannahs, *Physica C* 418 (2005) 160.
- [16] R.A. Ribeiro, S.L. Bud'ko, C. Petrovic, P.C. Canfield, *Physica C* 384 (2003) 227.
- [17] R.H.T. Wilke, S.L. Bud'ko, P.C. Canfield, D.K. Finnemore, S.T. Hannahs, *Physica C* 432 (2005) 193.
- [18] D.K. Finnemore, W.E. Straszheim, S.L. Bud'ko, P.C. Canfield, N.E. Anderson, R.J. Suplinskas, *Physica C* 385 (2003) 278.
- [19] R.H.T. Wilke, S.L. Bud'ko, P.C. Canfield, D.K. Finnemore, R.J. Suplinskas, S.T. Hannahs, *Physica C* 424 (2005) 1.
- [20] D.P. Whittle, J. Stringer, *Philos. Trans. R. Soc. London, Ser. A* 295 (1980) 309.
- [21] R.E. Carter, *J. Chem. Phys.* 34 (1961) 2010.